A Systematic Optimum Design of Waveguide-to-Microstrip Transition

Hong-bae Lee and Tatsuo Itoh, *Fellow, IEEE*

***Abstract*—In this paper, a systematic optimum design method is introduced, which consists of the finite-element method (FEM), design sensitivity analysis (DSA), and the steepest descent algorithm. A waveguide-to-microstrip (W/G-to-M/S) probe-type transition is designed by using the proposed method. In the FEM as a full-wave analyzer, eigenvalue and eigenvector calculations in the two-dimensional (2-D) FEM precedes the three-dimensional (3-D) FEM, in order to terminate the W/G-to-M/S transition model into an electrically small model. The analysis results of this approach are compared with ones of a commercial FEM software high-frequency structure simulator (HFSS). The total derivative required in the steepest descent algorithm is calculated numerically by the DSA based on the FEM. The additional time needed for this proposed method is only one more calculation of a sparse matrix equation. The return loss is chosen as the objective function to be minimized, and the backshort length and probe length are selected as the design variables in the transition design. The proposed method gives a good convergence characteristic and the optimized results show its usefulness.**

I. Introduction

There are many numerical methods based on full-wave analysis. The main goals of these methods are to achieve an optimum design of the given model. However, until now, these methods have been used to avoid the fabrication and performance evaluation phases of the intermediate products preceding the final design. In this use, the designer should change design parameters, depending on his or her experience, until the desired performance is achieved. It is very difficult even for an expert designer to do optimum design—especially if the structure is complex to the extent that it requires a full-wave analysis. This necessitates a systematic optimum design method in which only choosing objective function and design variables automatically gives an optimum design.

Extensive research of these schematic optimum designs [1]–[5] is being conducted. This research could be classified into two groups. One group includes the genetic algorithm [2], simulated annealing method [3], and evolution strategy [4], which uses the stochastic concepts in the direction-finding procedure. This stochastic concept makes convergence very slow and requires large amounts of the objective function evaluation. This large amounts make this research group impractical, especially in the design requiring full-wave analysis, even though it could get the global optimum. The other group uses the total derivative of the objective function with respect to design variables. This paper follows this idea and uses the steepest descent algorithm [6]. Since the relation between the objective function and design variables is expressed as an implicit function, the derivative required in this algorithm cannot be done analytically. Therefore, the design sensitivity analysis (DSA) is adopted.

The DSA is widely used in structural engineering [7]–[9] and in electromagnetic mechanics [10]–[12]. However, there is only a two-dimensional (2-D) application in microwave device design, as shown in [13], [14]. In this paper, the authors introduce a systematic design method which combines the DSA, the finite-element method (FEM), and the steepest descent algorithm for the three-dimensional (3-D) optimum waveguide-to-microstrip transition design. For the hermetic seal, the authors select probe-type transition as the model among the several transitions [15]–[17]. The FEM which is adopted as the full-wave analysis tool is preceded by the analytic (for the waveguide part) and the numerical (for the microstrip part) eigenvalue and eigenvector calculations in the 2-D application, in order to terminate the waveguide-to-microstrip (W/G-to-M/S) transition model into an electrically small one.

II. Finite-Element Method

The typical structure of waveguide-to-microstrip (W/G-to-M/S) consists of the transition part, waveguide part, and microstrip part, as shown in Fig. 1. The governing equation is easily obtained from the Maxwell's equation

$$\nabla \times \nabla \times \vec{E} + \mu\varepsilon \frac{\partial^2 \vec{E}}{\partial t^2} = 0. \tag{1}$$

With the assumption of time harmonic field and $e^{j\omega t}$ convention

$$\nabla \times \nabla \times \vec{E} - \omega^2 \mu\varepsilon \vec{E} = 0 \tag{2}$$

is derived. By applying Galerkin's method and simple vector identities, the following weak form is obtained:

$$\int \nabla \times \vec{W} \cdot \frac{\nabla \times \vec{E}}{\mu_r}\, dv - k^2 \varepsilon_r \int \vec{W} \cdot \vec{E}\, dv = \int \vec{W} \cdot \frac{\nabla \times \vec{E}}{\mu_r} \times \hat{n}\, ds. \tag{3}$$

Equation (3) consists of volume and surface integral terms. The edge element [18] is used, in order to use a divergence-free condition and the ease of imposing boundary condition

Manuscript received September 6, 1996; revised December 9, 1996. This work was supported by TRW under Subcontract HN4944RG5S under MAFET Thrust Area 2 Contract DAAL 01-95-C-3536.

The authors are with the Electrical Engineering Department, University of California at Los Angeles (UCLA), Los Angeles, CA 90095 USA.

Publisher Item Identifier S 0018-9480(97)03106-2.

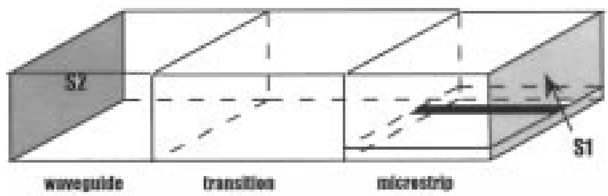

Fig. 1. W/G-to-M/S transition structure.

on it. The implementation of a volume integral with this edge element is well known. However, in order to truncate the analysis domain into the finite and smallest one, the discreet choice is needed on the surface integral treatment [19]. In this paper, the eigenvalues (corresponding to propagating constants) and eigenvectors are pre-calculated at surface S_1 and S_2 in Fig. 1. Since S_2 is an empty rectangular waveguide, those could be obtained analytically. Those at S_1 could be also obtained through the 2-D FEM [20]. These pre-calculated eigenvalues and eigenvectors could be combined through the surface integral term in (3). The final matrix equation can be expressed like (4) with the assumption that only one dominant mode is impinged on S_1:

$$\begin{bmatrix} [K_{00}] & [K_{01}] & [K_{02}] \\ [K_{10}] & [K_{11}]+[S_1] & [K_{12}] \\ [K_{20}] & [K_{21}] & [K_{22}]+[S_2] \end{bmatrix} \begin{bmatrix} [E_0] \\ [E_{t1}] \\ [E_{t2}] \end{bmatrix} = \begin{bmatrix} [0] \\ [\tilde{e}_t^{\rm inc}] \\ [0] \end{bmatrix}. \tag{4}$$

In (4), $[E_0]$, $[E_{t1}]$, and $[E_{t2}]$ are the electric-field intensities at edges in the volume inside, and on the surfaces S_1 and S_2, respectively. The submatrices [21], [22] are given as follows:

$$[K] = \sum_e \left[\sum_{j=1}^{N_e} \int \nabla \times \vec{W}_i \cdot \frac{\nabla \times \vec{W}_j}{\mu_r}\, dv - k^2 \varepsilon_r \int \vec{W}_i \cdot \vec{W}_j \, dv \right], \qquad i = 1, \cdots, N_e \tag{5}$$

$$[S_1] = \sum_{m=0}^{\infty} \frac{s_m |\gamma_m|}{k_0} \gamma_m \{\tilde{e}_t\}_m \{\tilde{e}_t\}_m^+ \tag{6}$$

$$[S_2] = \sum_e \int \vec{W}_i \cdot \left\{ \sum_{m,n} \frac{k_0^2}{\gamma_{mn}} e_{tmn}^{\rm TM} \left[\sum_e \sum_{j=1}^{N_e} \int e_{tmn}^{\rm TM} \cdot \vec{W}_j \, ds' \right] - \sum_{m,n} \gamma_{mn} e_{mn}^{\rm TE} \left[\sum_e \sum_{j=1}^{N_e} \int e_{mn}^{\rm TE} \cdot \vec{W}_j \, ds' \right] \right\} ds \tag{7}$$

$$[\tilde{e}_t^{inc}] = 2\gamma_0 e^{-\gamma_0 z_1} \{\tilde{e}_t\}_0. \tag{8}$$

For further detail, see [21], [22]. As expressed in (6)–(8), the surface integral term in (3) can be implemented with pre-calculated eigenvalues (γ_m and $\gamma_{m,n}$) and eigenvectors ($\{\tilde{e}_t\}_m$, $e_{tmn}^{\rm TM}$, and $e_{mn}^{\rm TE}$).

III. Design Sensitivity Analysis

The FEM eventually makes the matrix equation like (4) which can be rewritten as

$$K(b)z = F(b) \tag{9}$$

where $K(b)$ [number of state variable ($n\_{\rm state}$) $\times$ $n\_{\rm state}$] is the global (reduced) stiffness matrix, $F(b)$ [$n\_{\rm state} \times 1$] is the load, b [number of design variable ($n\_{\rm var}$) $\times$ 1] is the design variable vector, and z [$n\_{\rm state} \times 1$] is the state variable vector.

The design variable vector b could be a shape, material constants, or size. In the design problem, the object (cost) function to be minimized could be expressed as a general form:

$$\Psi = \Psi[b, z(b)]. \tag{10}$$

The (10) means the objective function is the implicit function of design variables. Therefore, the total derivative with respect to design could be given as the following equation:

$$\frac{d\Psi}{db} = \frac{\partial \Psi}{\partial b} + \frac{\partial \Psi}{\partial z} \cdot \frac{dz}{db} \tag{11}$$

where

$$\frac{d\Psi}{db} = \left[\frac{d\Psi}{db_1}, \cdots, \frac{d\Psi}{db_{n\_{\rm var}}} \right]$$

$$\frac{d\Psi}{dz} = \left[\frac{d\Psi}{dz_1}, \cdots, \frac{d\Psi}{dz_{n\_{\rm state}}} \right]$$

and

$$\frac{dz}{db} = \begin{bmatrix} \dfrac{dz_1}{db_1} & \cdots & \dfrac{dz_1}{db_{n\_{\rm var}}} \\ \vdots & \vdots & \vdots \\ \dfrac{dz_{n\_{\rm state}}}{db_1} & \cdots & \dfrac{dz_{n\_{\rm state}}}{db_{n\_{\rm var}}} \end{bmatrix}.$$

Unlike the partial derivative terms in (11), the total derivative of the state variable with respect to the design variable vector is not easily obtained, since the relation between the state and the design variables is implicit. However, by differentiating both sides of (9), one obtains the following equation:

$$K(b) \frac{dz}{db} + \frac{\partial K(b)}{\partial b} \cdot z = \frac{\partial F(b)}{\partial b} \tag{12}$$

where

$$\frac{\partial F(b)}{\partial b} = \begin{bmatrix} \dfrac{\partial F_1}{\partial b_1} & \cdots & \dfrac{\partial F_1}{\partial b_{n\_{\rm var}}} \\ \vdots & \vdots & \vdots \\ \dfrac{\partial F_{n\_{\rm state}}}{\partial b_1} & \cdots & \dfrac{\partial F_{n\_{\rm state}}}{\partial b_{n\_{\rm var}}} \end{bmatrix}.$$

By putting (12) into (11), one can get the total derivative equation

$$\frac{d\Psi}{db} = \frac{\partial \Psi}{\partial b} + \frac{\partial \Psi}{\partial z} \cdot K(b)^{-1} \frac{\partial}{\partial b} [F(b) - K(b)\tilde{z}] \tag{13}$$

where $\tilde{z}$ denotes the constant with respect to design.

Equation (13) includes an inverse matrix calculation and the direct calculation of the inverse of a large matrix requires a large amount of computation time. The introduction of the adjoint variable vector ($\lambda[n\_\mathrm{state} \times 1]$) defined as

$$\lambda \equiv \left[\frac{\partial \Psi}{\partial z} K(b)^{-1}\right]^T = K(b)^{-T} \frac{\partial \Psi^T}{\partial z} \tag{14}$$

can overcome this difficulty. By using the symmetry of stiffness matrix, (14) can be rewritten as

$$K(b)\lambda = \frac{\partial \Psi^T}{\partial z}. \tag{15}$$

Solving (15) gives the adjoint variable vector. By replacing (13) with this calculated adjoint variable vector, the final total derivative can be obtained:

$$\frac{d\Psi}{db} = \frac{\partial \Psi}{\partial b} + \lambda^T \frac{\partial}{\partial b}[F(b) - K(b)\tilde{z}]. \tag{16}$$

As shown in (16), there are only partial derivatives. Therefore, the additional computation to get the total derivative is to calculate (15). Since (9) and (15) have the same stiffness matrix, one can save the time for the making of the stiffness matrix. Obtaining the total derivative through the DSA means finding the direction to which the design variables have to move to get the minimum value of the objective function. The remaining part is how to update the design systematically. In this step, the steepest descent algorithm is adopted. For this algorithm, one defines the normalized direction vector ($s[n\_\mathrm{var} \times 1]$):

$$s = \frac{\frac{d\Psi}{db}}{\left\|\frac{d\Psi}{db}\right\|}. \tag{17}$$

If one assumes that the objective function value is zero at the updated design, one can get the useful equation with the Taylor expansion:

$$\Psi(b + ls) = \Psi(b) + \frac{d\Psi}{db} \cdot ls^T + \mathrm{h.o.t} = 0. \tag{18}$$

By neglecting the higher order terms, one can get the step length:

$$l = \frac{-\Psi(b)}{\left\|\frac{d\Psi}{db}\right\|}. \tag{19}$$

Since the higher order terms are neglected, one has to get to the optimum point iteratively. With the step length and the normalized direction, the design could be updated systematically:

$$b^{\mathrm{new}} = b^{\mathrm{old}} + ls. \tag{20}$$

The design procedure introduced in this paper with the FEM, the DSA, and the steepest descent method is summarized in Fig. 2.

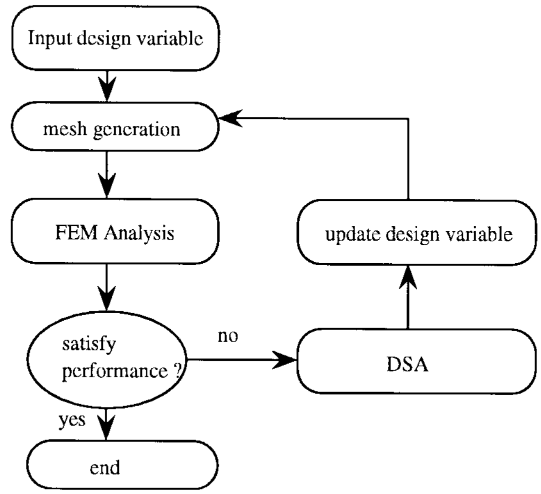

Fig. 2. Design procedure of the proposed method.

IV. Numerical Results

The systematic design method introduced in this paper is applied to a probe-type transition structure design. Fig. 3 shows the design model intended for use with the hermetic seal. The specifications are shown in Table I. Due to the fact that this structure has no curvilinear surface and the fact that meshing is easy with the rectangular element, the authors use the brick edge element. While the edge element causes no spurious solution, it cannot guarantee the positive definite stiffness matrix. Therefore, the authors use the preconditioning quasiminimal residual (QMR) method as a large sparse matrix solver. To verify the accuracy of the proposed FEM which uses the precalculated 2-D eigenvalues and eigenvectors, the return loss is calculated. The return loss at S_1 can be defined [22] as

$$S_{11} = \frac{|\gamma_0|}{k_0}\{\tilde{e}_t\}^+ E_t - 1 \tag{21}$$

where $+$ means Hermitian.

The results compared with a commercial FEM package, high-frequency structure simulator (HFSS), are shown in Fig. 4. For this analysis, the authors use 1600 brick edge elements and 5786 edges, while HFSS uses 4228 tetrahedral elements and 23 768 edges. As shown in Fig. 4, the graphs closely correlate.

In this type transition, the backshort location and probe length are important factors for broad-band applications [23]. However, for the test of the DSA, only one parameter [the back short length (l)] is selected as the design variable first. The authors define the $|S_{11}|^2$ as the objective function to be minimized. Then the objective function (Ψ) can be expressed with respect to (21) as

$$\Psi = \mathrm{Re}\left[\frac{|\gamma_0|}{k_0}\{\tilde{e}_t\}^+ E_t - 1\right]^2 + \mathrm{Im}\left[\frac{|\gamma_0|}{k_0}\{\tilde{e}_t\}^+\{E_t\} - 1\right]^2. \tag{22}$$

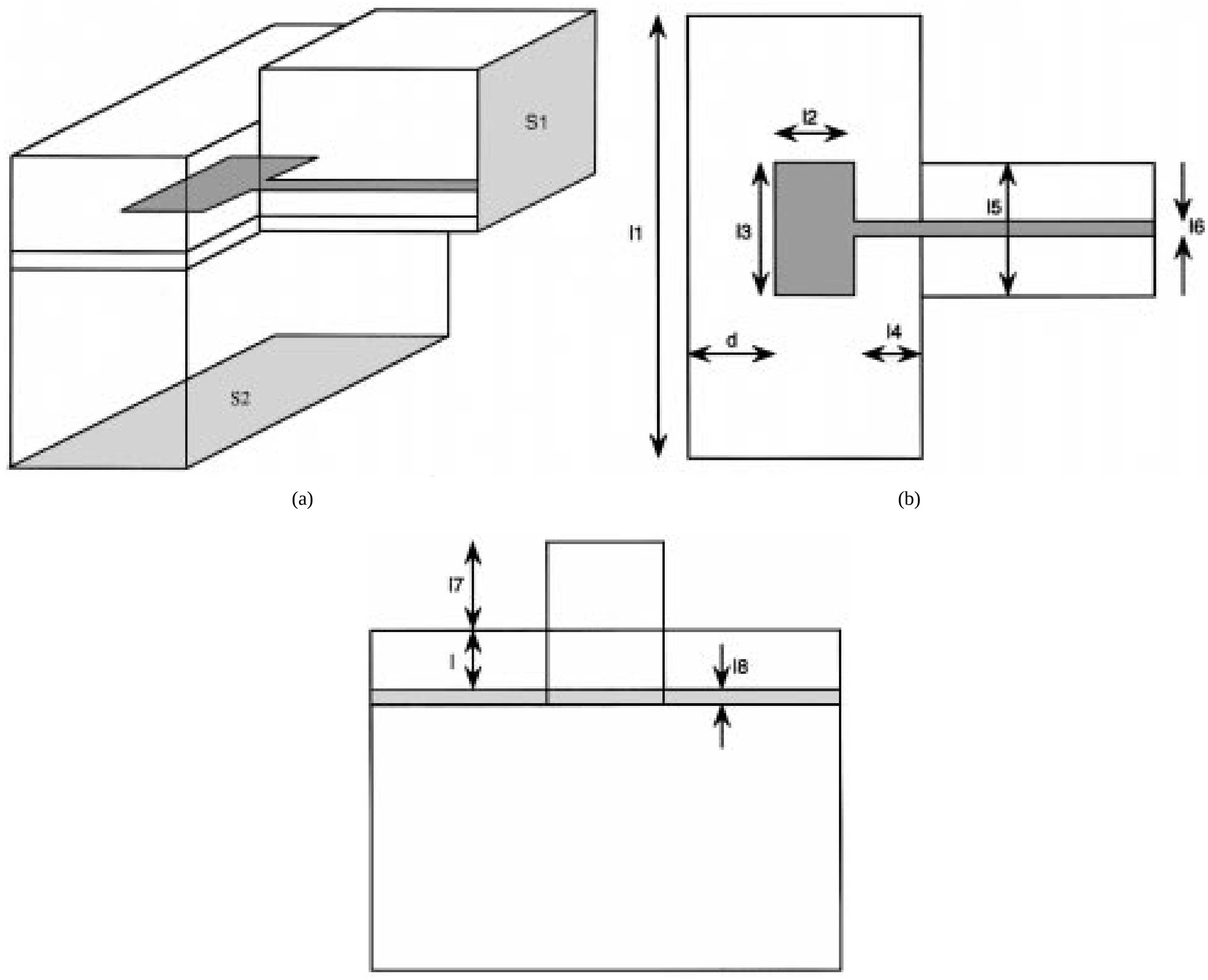

Fig. 3. (a) Probe type W/G-to-M/S transition. (b) Top view. (c) Side view.

Then the total derivative of the objective function with respect to design variable is derived as

$$\frac{d\Psi}{db} = \mathrm{Re}\left[2 \cdot \left(\frac{|\gamma_0|}{k_0}\{\tilde{e}_t\}^+\{E_t\} - 1\right)^* \cdot \frac{d}{db}\left(\frac{|\gamma_0|}{k_0}\{\tilde{e}_t\}^+\{E_t\} - 1\right)\right]. \quad (23)$$

The total derivative expressed in terms of S_{11} is

$$\frac{d\Psi}{db} = \mathrm{Re}\left(2 \cdot S_{11}^* \cdot \left\{\frac{\partial S_{11}}{\partial b} + \lambda^T \frac{\partial}{\partial b}[F(b) - K(b)\tilde{z}]\right\}\right) \quad (24)$$

where * signifies the complex conjugate.

From the facts that S_{11} and $F(b)$ are defined on S_1 while the design variable is inside the transition, the partial derivatives involved with these two functions should be zero. This makes (24) more simple:

$$\frac{d\Psi}{db} = -\mathrm{Re}\left\{2 \cdot S_{11}^* \cdot \left[\lambda^T \cdot \frac{\partial}{\partial b} K(b)\tilde{z}\right]\right\}. \quad (25)$$

And the adjoint variable vector is obtained from

$$K(b)\lambda = \left(\frac{\partial S_{11}}{\partial z}\right)^T. \quad (26)$$

Fig. 5 shows the objective function values and their sensitivities with varying backshort length at a fixed frequency of 40 GHz. As shown in Fig. 5, the objective function value has its minimum between 35–40 mL. Therefore, the optimum backshort length should be between these two values. Also, the change of the sign of the sensitivity is observed in that region. Farther from this region, the absolute value of the sensitivity increases. Compared with the objective function pattern in Fig. 5, this sensitivity characteristic is expected. Fig. 6 shows the step lengths calculated by (19). It means, for example, the shortback length (l) should move about 7 mL farther to get the optimum performance when l is 21.6 mL. Since the higher order terms in obtaining the step length were neglected, one should do it iteratively. Fig. 7 gives the convergence characteristics of the proposed design method. In this case, the initial shortback length is chosen as 46.6 mL, and

TABLE I
SPECIFICATIONS OF THE TRANSITION

[unit : mil]

d	l	l1	l2	l3	l4	l5	l6	l7	l8
60	39	224	42	50	10	50	7.4	27.6	7.4

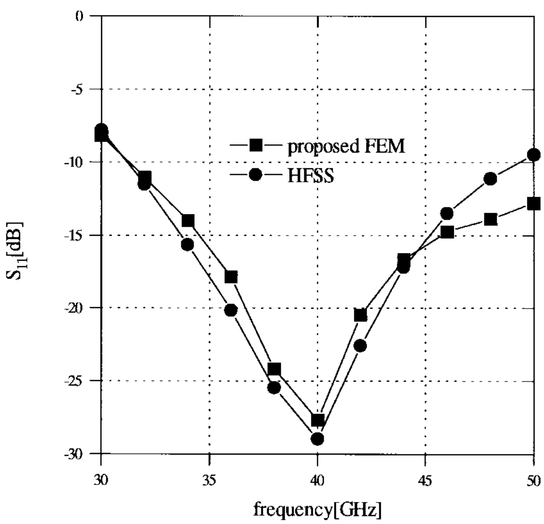

Fig. 4. Analysis results from the proposed FEM and HFSS.

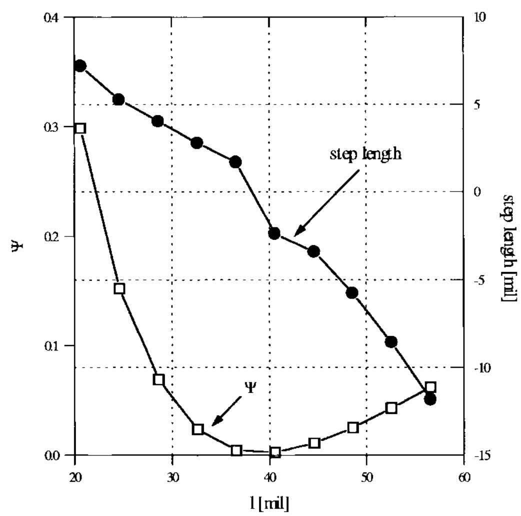

Fig. 6. Step length variation.

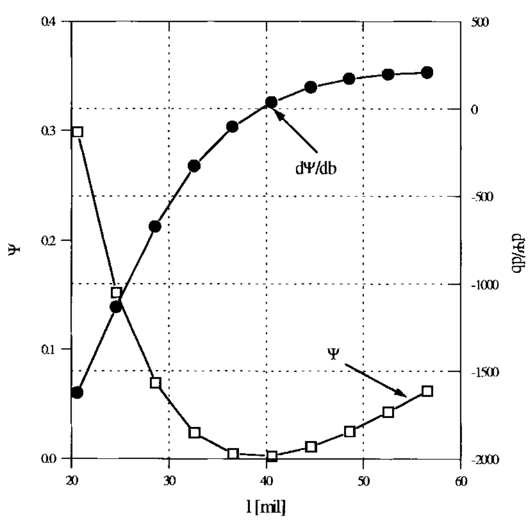

Fig. 5. Calculated sensitivity in the test model.

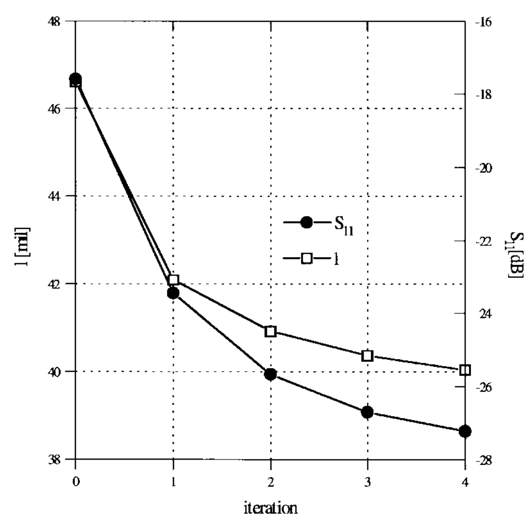

Fig. 7. Convergence characteristics of the test model.

the design process is stopped if the calculated step length is less than 1 mL. Therefore, convergence in the fourth iteration as shown in Fig. 7 means the total number of large sparse matrix calculation is 10. Fig. 7 also shows the improvement of the return losses in dB from about 18 dB to about 27 dB. For the real design, the backshort length and probe length as design variables are selected, and are optimized at 45 GHz. The convergence of design variables and objective function are shown in Figs. 8 and 9. While the backshort length is changed considerably through the design process, the probe length remains almost constant. This means the probe length is not critical in this type of transition. S_{11} is also improved as shown in Fig. 9. Even though the transition was designed at 45 GHz, the improvement of frequency response is also obtained as shown in Fig. 10.

V. CONCLUSION

In this paper, a systematic design method is introduced. This method consists of the FEM, the DSA, and the steepest descent

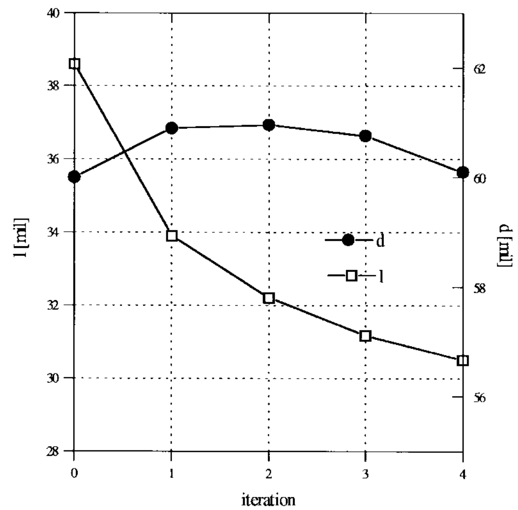

Fig. 8. Convergence characteristics of design variables.

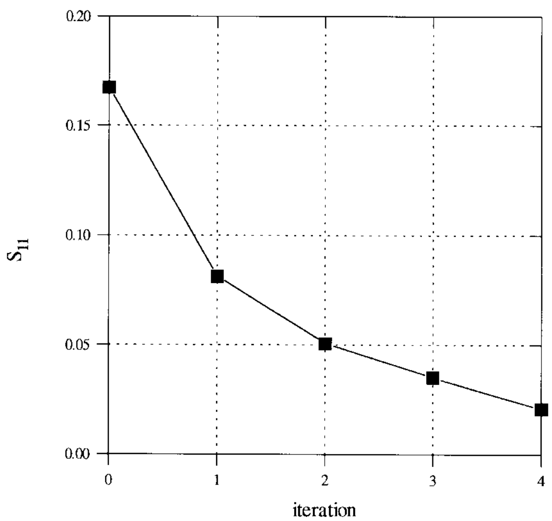

Fig. 9. Convergence of objective function.

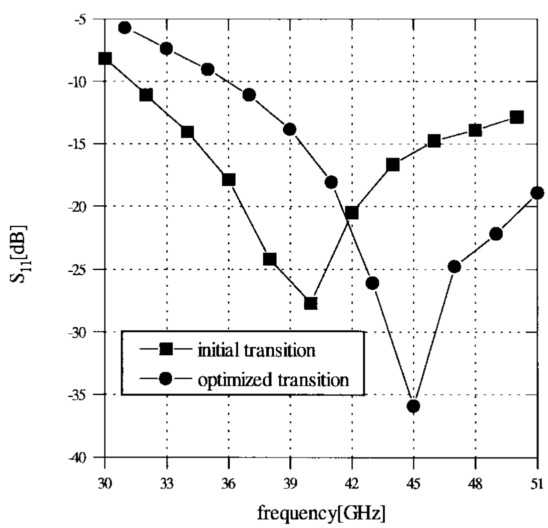

Fig. 10. Comparison of optimized and initial transition.

method. The FEM with 2-D eigenvalues and eigenvectors reduced the matrix size. The results applied to the W/G-to-M/S transition analysis were compared with ones from HFSS with both showing similar results. In order to get some characteristics of the proposed method, only one parameter (backshort length of W/G-to-M/S transition) was chosen as the design variable first, and S_{11} was minimized. The result gave a good explanation about the proposed design method. After testing, the backshort length and probe length were selected as design variables. The optimum values were obtained and it was found that the probe length is not critical. Even though only a closed structure with two ports was dealt with in this paper, this method could also be directly applied to other structures. This proposed method could easily be expanded to a shape design problem because there is no extra time needed for the increase of the design variables. Since the DSA starts with a matrix equation, replacing the FEM with other methods which results in a matrix equation, can give other good systematic design methods.

References

[1] E. J. Haug, K. K. Choi, and V. Komkov, *Design Sensitivity Analysis of Structural Systems.* New York: Academic, 1986.

[2] F. Thollon and N. Burais, "Genetical optimization for sensors for eddy currents. Nondestructive testing and evaluation," *IEEE Trans. Magn.*, vol. 31, pp. 2026–2031, May 1995.

[3] E. H. L. Aarts, *Simulated Annealing and Boltzmann Machines: A Stochastic Approach to Combinatorial Optimization and Neural Computing.* New York: Wiley, 1989.

[4] M. Kasper, "Shape optimization by evolution strategy," *IEEE Trans. Magn.*, vol. 28, pp. 1556–1560, Mar. 1992.

[5] H.-b. Lee, "Computer aided optimal design methods for waveguide structures," Ph.D. dissertation, Dept. of Electrical Engineering, Seoul National Univ., Seoul, Korea, 1995.

[6] J. S. Arora and E. J. Haug, "Effective optimal design of structures by generalized steepest descent programming," *Int. J. Numer. Methods Eng.*, vol. 10, pp. 747–766, 1976.

[7] E. J. Haug and J. Cea, *Optimization of Distributed Parameters Structures: Vols. I and II.* The Netherlands: Sijhoff & Noordhiff, 1981.

[8] O. Paronneaum, *Optimal Shape Design for Elliptic Systems.* Berlin, Germany: Springer-Verlag, 1983.

[9] S. Y. Wang, Y. B. Sun, and R. H. Gallagher, "Sensitivity analysis in shape optimization of continuum structures," *Comput. Struc.*, vol. 20, no. 5, pp. 855–867, 1985.

[10] I. H. Park, B. T. Lee, and S. Y. Hahn, "Pole shape optimization for reduction of cogging torque by sensitivity analysis," *COMPEL*, vol. 9, suppl. A, pp. 111–114, 1990.

[11] C. S. Koh, "Optimal shape design of electric apparatus using design sensitivity analysis," Ph.D. dissertation, Dept. of Electrical Engineering, Seoul National Univ., Seoul, Korea, 1992.

[12] S. Gitosusastro, J. L. Coulomb, and J. C. Sabonnadiere, "Performance derivative calculation and optimization," *IEEE Trans. Magn.*, vol. 25, pp. 2834–2839, July 1989.

[13] H. B. Lee, H. K. Jung, and S. Y. Hahn, "Shape optimization of *H*-plane waveguide tee junction using edge finite element method," *IEEE Trans. Magn.*, vol. 31, pp. 1928–1931, May 1995.

[14] J. Kim, H. B. Lee, H. K. Jung, and S. Y. Hahn, "Optimal design technique for waveguide device," *IEEE Trans. Magn.*, vol. 32, pt. 1, pp. 1250–1253, May 1996.

[15] T. Q. Ho and Y. Shih, "Spectral-domain analysis of *E*-plane waveguide to microstrip transition," *IEEE Trans. Microwave Theory Tech.*, vol. 37, pp. 388–392, Feb. 1989.

[16] W. Grabherr, B. Huder, and W. Menzel, "Microstrip to waveguide transition compatible with MM-wave integrated circuits," *IEEE Trans. Microwave Theory Tech.*, vol. 42, pp. 1842–1843, Sept. 1994.

[17] W. Menzel and A. Klaassen, "On the transition from ridged waveguide to microstrip," in *Proc. 19th European Microwave Conf.*, London, U.K., Sept. 1989, pp. 1265–1269.

[18] A. Bossavit, "Whitney forms: A class of finite elements for three dimensional computations in electromagnetism," *Proc. Inst. Elect. Eng.*, vol. 135, pt. A, pp. 493–500, Nov. 1988.

[19] T. Itoh, G. Pelosi, and P. Silvester, *Finite Element Software for Microwave Engineering.* New York: Wiley, 1996, pp. 267–312.

[20] M. S. Alam, K. Hirayama, Y. Hayashi, and M. Koshiba, "A vector finite-element analysis of complex modes in shielded microstrip lines," *Microwave Opt. Tech. Lett.*, vol. 6, no. 16, pp. 873–875, Dec. 1993.

[21] J. Jin, *The Finite Element Method in Electromagnetics.* New York: Wiley, 1993, pp. 357–361.

[22] K. Hirayama, M. S. Alam, Y. Hayashi, and M. Koshiba, "Vector finite element method with mixed-interpolation-type triangular-prism element for waveguide discontinuities," *IEEE Trans. Microwave Theory Tech.*, vol. 42, pp. 2311–2316, Dec. 1994.

[23] Y. C. Shih, T. N. Ton, and L. Q. Bui, "Waveguide-to-microstrip transitions for millimeter-wave applications," in *IEEE MTT-S Dig.*, New York, May 1988, pp. 473–475.

Hong-bae Lee (M'96) was born on August 11, 1966, in Seoul, Korea. He received the B.S., M.S., and Ph.D. degrees, all in electrical engineering, from Seoul National University, Seoul, Korea, in 1989, 1991, and 1995, respectively.

From March 1995 to February 1996, he was a Researcher of EESRI at Seoul National University. He is currently a Post-Doctoral Fellow with the Electrical Engineering Department, University of California at Los Angeles (UCLA), Los Angeles, CA. His current research interests include the numerical methods for microwave and millimeter-waves devices, optimum design based on the full-wave analysis, actuator design, and active circuit design with full-wave analysis.

Tatsuo Itoh (S'69–M'69–SM'74–F'82) received the B.S. and M.S. degrees from Yokohama National University, Japan, and the Ph.D. degree in electrical engineering from the University of Illinois, Urbana in 1964, 1966, and 1969, respectively.

From September 1966 to April 1976, he was with the Electrical Engineering Department, University of Illinois. From April 1976 to August 1977, he was a Senior Research Engineer in the Radio Physics Laboratory, SRI International, Menlo Park, CA. From August 1977 to June 1978, he was an Associate Professor at the University of Kentucky, Lexington. In July 1978, he joined the faculty at The University of Texas at Austin, where he became a Professor of electrical engineering in 1981 and Director of the Electrical Engineering Research Laboratory in 1984. During the summer of 1979, he was a guest Researcher at AEG-Telefunken, Ulm, West Germany. In September 1983, he was selected to hold the Hayden Head Centennial Professorship of Engineering at The University of Texas. In September 1984, he was appointed Associate Chairman for Research and Planning of the Electrical and Computer Engineering Department at The University of Texas. In January 1991, he joined the University of California at Los Angeles (UCLA) as Professor of electrical engineering and Holder of the TRW Endowed Chair in microwave and millimeter wave electronics. He is currently the Director of the Joint Services Electronics Program (JSEP) and Director of the Multidisciplinary University Research Initiative (MURI) program at UCLA. He was an Honorary Visiting Professor at Nanjin Institute of Technology, China, as well as at the Japan Defense Academy. In April 1994, he was appointed an Adjunct Research Officer for Communications Research Laboratory, Ministry of Post and Telecommunication, Japan. He currently holds a Visiting Professorship at the University of Leeds, U.K., and is an External Examiner of the graduate program of City University of Hong Kong.

Dr. Itoh is a member of the Institute of Electronics and Communication Engineers of Japan, and Commissions B and D of USNC/URSI. He served as the Editor of IEEE TRANSACTIONS ON MICROWAVE THEORY AND TECHNIQUES from 1983 to 1985. He serves on the Administrative Committee of IEEE Microwave Theory and Techniques Society. He was Vice President of the Microwave Theory and Techniques Society in 1989 and President in 1990. He was the Editor-in-Chief of IEEE MICROWAVE AND GUIDED WAVE LETTERS from 1991 through 1994. He was elected as an honorary life member of the MTT Society in 1994. He was the Chairman of USNC/URSI Commission D from 1988 to 1990, the Vice Chairman of Commission D of the International URSI from 1991 to 1993 and is currently Chairman of the same Commission. From 1993 to 1996, he was on the Long Range Planning Committee of URSI. He serves on advisory boards and committees of a number of organizations including the National Research Council and the Institute of Mobile and Satellite Communication, Germany.